

# Landslides and glacier retreat at Mt. Meager volcano: hazard and risk challenges



Roberti G.<sup>1,2</sup>, Ward B.<sup>2</sup>, van Wyk de Vries B.<sup>1</sup>, Falorni G.<sup>3</sup>, Menounos B.<sup>4</sup>, Friele P.<sup>5</sup>, Williams-Jones G.<sup>2</sup>, Clague J.J.<sup>2</sup>, Perotti G.<sup>6</sup>, Giardino M.<sup>6</sup>, Baldeon, G.<sup>3</sup>, Freschi S.<sup>6</sup>

1 *Laboratoire Magmas et Volcans, CNRS, IRD, OPGC - Université Clermont Auvergne, Campus Universitaire des C zeaux, 6 Avenue Blaise Pascal, TSA 60026 - CS 60026, 63178 Aubiere Cedex, France*

2 *Earth Sciences Department - Simon Fraser University, 8888 University Drive, Burnaby, British Columbia V5A 1S6, Canada*

3 *TRE-ALTAMIRA Inc., 475 W Georgia Street, Suite 410, Vancouver, British Columbia, V6B 3A3, Canada*

4 *Geography Program and Natural Resources and Environmental Studies Institute - University of Northern British Columbia, 3333 University Way, Prince George, British Columbia, V2N 4Z9, Canada*

5 *Cordilleran Geoscience, PO Box 612, Squamish, British Columbia V8B 0A5, Canada*

6 *Earth Sciences Department, GeoSitLab - GIS and Geomatics Laboratory - University of Torino, Via Valperga Caluso 35, Torino, 10125, Italy*

## ABSTRACT

Mt. Meager is a glacier-clad volcanic complex in southwest British Columbia. In the summer of 2010, melting snow and ice caused by warm weather triggered the collapse of 53 Mm<sup>3</sup> of rock and debris from Mt. Meager's south flank, generating the largest historic landslide in Canada. In 2016 fumaroles formed ice caves in one of its glaciers, raising concern about the potential for eruptive activity. Following these events, we carried out a geomorphic study of the volcano. Employing satellite-based differencing methods, we measured movements on previously identified unstable slopes and documented the recent retreat of glaciers on the volcanic complex. It is likely that glaciers will continue to thin and recede, and that slopes will continue to deform, possibly leading to catastrophic collapses similar to the 2010 event. Previous work concluded that the level of risk posed by large landslides at Mt. Meager is unacceptable. In spite of this conclusion, little has been done to manage the risk by local or provincial governments over the past decade. With new hydropower infrastructure near the volcano and continued population growth in the Lillooet River valley downstream, it is clear that the landslide risk is increasing.

## R SUM 

Mt. Meager est un complexe volcanique recouvert de glaciers en Colombie-Britannique. Dans l' t  2010, la fonte de neige et la glace a provoqu  l'effondrement de 53 Mm<sup>3</sup> de roches et de d bris du flanc sud de Mt. Meager, g n rant le plus grand glissement de terrain historique au Canada; en 2016 fumarolles ont form  des grottes dans l'un de ses glaciers. Suite   ces  v nements, nous avons r alis  une  tude g omorphologique du volcan. Nous avons identifi  des pentes instables et caract ris  la retraite glaciaire sur le complexe volcanique. La perte de glace se poursuivra et le mouvement des pentes s'accr l rera, ce qui pourrait mener   des effondrements catastrophiques comme en 2010. Des travaux ant rieurs ont conclu que le niveau de risque pos  par les glissements de terrain au Mt. Meager est inacceptable, mais les autorit s locales ont peu fait pour g rer les risques. Avec la croissance continue des communaut s et des infrastructures pr s du volcan, la perception soci tale de ce risque doit changer.

## 1 INTRODUCTION

Mt. Meager is a volcanic complex in southwest British Columbia, Canada, about 150 km north of Vancouver and 65 km northwest of the town of Pemberton. The volcanic complex formed over the past two million of years (Read 1978) and last erupted about 2400 years ago (Clague et al. 1995; Hickson et al. 1999). Today, it hosts an active hydrothermal system and fumarole field (Venugopal et al. 2017) and it is a site of shallow earthquakes (Friele et al. 2008). It was periodically covered by glaciers during the Pleistocene Epoch (Clague and Ward 2011), and

presently supports alpine glaciers (Holm et al. 2004, Koch et al. 2009). The volcano has a long record of landslides (Friele et al. 2008), stemming from extensive hydrothermal alteration of the volcanic rocks, glacial erosion, and recent glacier retreat (Holm et al. 2004, Roberti et al. 2017c). The most recent large landslide, in 2010, is the largest in Canadian history (Roberti et al. 2017c). Glacier retreat has also exposed hydrothermal vents at Mt. Meager, affecting water circulation, temperature, and chemistry. In 2016, fumaroles formed

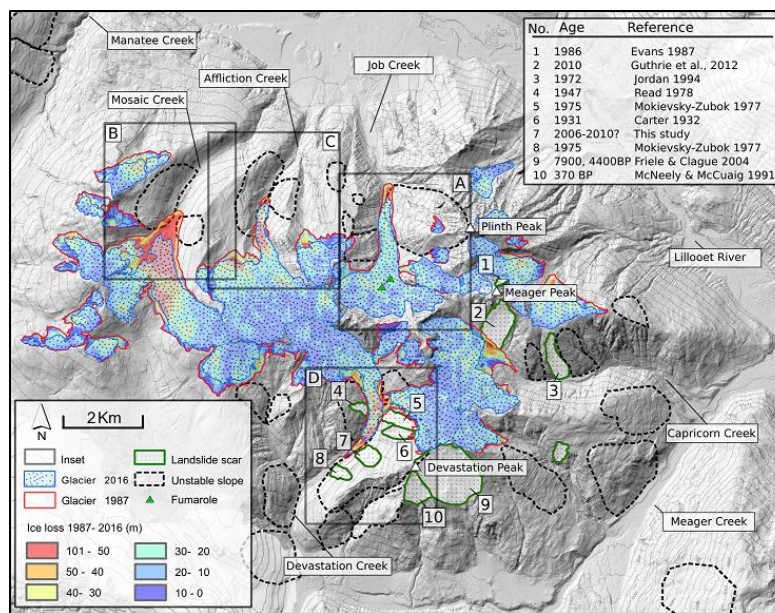


Figure 1. Overview of the Mt. Meager volcanic complex, showing glaciers, ice loss, fumaroles, past landslides, unstable slopes. A) Figure 2. B) Figure 3. C) Figure 4, D) Figure 5.

ice caves in Job Glacier on the north side of Mt. Meager. The basin of Job Creek is also one of the most unstable catchments on the massif and the source of some of its largest ( $10^8$ - $10^9$  m<sup>3</sup>) prehistoric landslides (Friele et al. 2008).

Many studies have focused on the stability of Mt. Meager (Jordan 1994, Jakob 1996, Friele and Clague 2004, Holm et al. 2004, Friele et al. 2005, Simpson et al. 2006). Friele et al. (2008) quantified the debris flow risk to residents and infrastructure in the Lillooet river valley, 32-75 km downstream from the volcano. In light of international standards (Leroi et al. 2005), they deemed the risk to be unacceptable, but little mitigation by local authorities (e.g., education, land zoning) has been done. Meanwhile, two hydropower plants have been built at the foot of the volcano, and a new access road for forestry operations in Meager Creek valley, just south of Mt. Meager, is being constructed. There are active mining operations on the east flank of the volcano, and the population in the Lillooet River valley is rapidly growing (Statistics Canada 2017).

Although previous researchers have recognized the importance of glacier retreat on slope stability at Mt. Meager, we are far from a complete understanding of the effects of deglaciation on the volcanic system, notably in terms of stability, hydrothermal circulation and relations between the two. Here we present a geomorphic study of the Mt. Meager Volcanic Complex, with a focus on major slope instabilities and recent glacier retreat. We discuss volcanic and landslide hazards in relation to a previous risk analyses (Friele et al. 2008). Finally, we suggest a monitoring framework for the volcanic massif.

## 2 METHODS

We used remote sensing methods and site-specific field work to map and describe landslide and glacial activity at Mt Meager. We applied Structure from Motion (SfM) photogrammetric methods to British Columbia Provincial Government vertical aerial photographs to produce orthophotos of the volcano. Lidar (Light detection and ranging) data were acquired in 2015 and 2016, from which we produced an up-to-date digital elevation model (DEM). Interferometric Synthetic Aperture Radar (InSAR) analysis was carried out to identify unstable slopes and constrain deformation rates. Comparison of the 2015-2016 Lidar-derived DEM and a DEM resulting from the 1987 British Columbia Terrain Resource Inventory Map (TRIM) allowed us to document nearly three decades of glacier retreat on the volcanic massif.

### 2.1 Structure from Motion

SfM is a photogrammetry technique based on computing vision algorithms (Carrivick et al. 2016). The use of SfM has rapidly increased in the last few years, rivaling Lidar as a tool for acquiring high-resolution topography (Westoby et al. 2012; Fonstad et al. 2013). SfM is generally applied to photographs taken with a hand-held camera or from an Unmanned Aircraft Vehicle (UAV) (James and Robson 2012). In comparison, few studies have explored the application of Structure from Motion (SfM) to digitized historical vertical aerial photographs (Gomez et al. 2015; Bakker and Lane 2016; Roberti et al. 2017b). In this study we processed 114 British Columbia Government vertical aerial photographs acquired in the summer of 2006 (see Roberti et al. 2017c for details on data processing). Part of this dataset was used by Roberti et al. (2017c) to constrain slope deformation prior the

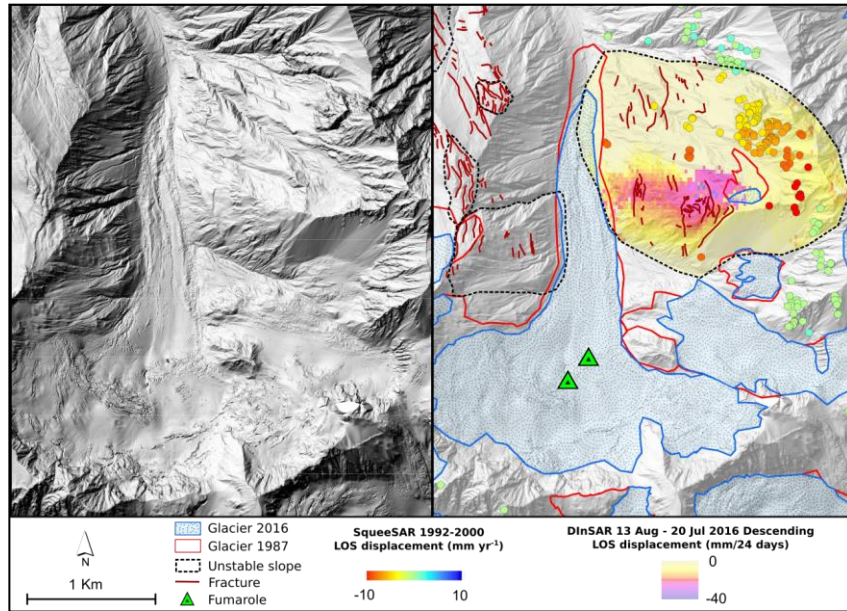


Figure 2. Job Creek valley (Inset A, Figure 1), showing past and present glacier outlines, unstable slopes, fractures, and fumaroles. SqueeSAR displacement data, and DInSAR deformation map are also shown. The volume estimate of the unstable slopes is  $10^8$ - $10^9$  m<sup>3</sup>. LOS = line of sight

2010 Mt Meager landslide and constrain the volume of the landslide.

## 2.2 Lidar

Aerial Lidar technology enables acquisition of high-resolution topographic data over large areas. Vegetation can be automatically removed to produce 'bare-earth' DEMs suitable for geomorphic analysis. Lidar covering the Mt. Meager Volcanic Complex was acquired during summer 2015 and 2016 with a Riegl VQ-580 scanner equipped with an Applanix POS AV910 inertial measurement unit/GNSS receiver for geolocation and orientation of the scanner relative to the surveyed terrain. The Southern sector of the volcano was surveyed in 2015 whereas the Northern half of the volcano was surveyed in 2016. Point cloud density averaged 2.57 points m<sup>-2</sup>, and we generated 1 m terrain models from these data. Slope, aspect and shaded relief maps were then generated from the DEM

## 2.3 Interferometric Synthetic Aperture Radar

Satellite-based InSAR methods allow measurement of displacement with millimetric precision over large areas (Ferretti et al. 2015). The first radar satellites were launched in the 1990s and the number of available satellite systems continues to increase. In this study, we used freely available radar satellite images from the European Space Agency (ESA) ERS 1-2 and Sentinel-1 constellations. The ERS 1-2 data set consists of 33 images spanning the period June 3<sup>rd</sup> 1992 to September 23<sup>rd</sup> 2000 with a nominal 35-day revisit frequency. The imagery was acquired from satellite track 471, along a descending orbit with a 24.9° look angle and 5.6 cm

wavelength. Acquisitions from the Sentinel-1 satellites started in late 2014 and are currently continuing with a 12-day revisit frequency. Three separate data sets are being acquired from both ascending and descending orbits.

We processed the ERS data set with the SqueeSAR algorithm (Ferretti et al., 2011), which identifies point targets (Permanent Scatterers, PS) and distributed scatterers (DS), to produce a point cloud with high precision measurements of displacement. The analysis produced 3,182 measurement points (MP) over the 313 km<sup>2</sup> of Mt Meager area, leading to a point density of 10 MP km<sup>-2</sup>.

The Sentinel imagery is being used to generate differential interferograms (DInSAR) and produce displacement maps over the Mt. Meager massif. DInSAR identifies changes in signal phase between pairs of SAR images and, coupled with a high-resolution DEM, allows the measurement of ground displacement that occurs in the period between the two image acquisition dates with ± 10 mm precision. As InSAR is hindered by the presence of vegetation and snow cover the best results are obtained by comparing images acquired during the summer or early fall. This approach provides the best results in terms of spatial coverage but does not allow detection of deformation over long periods of time nor does it provide the deformation history that can be obtained with the SqueeSAR approach.

## 2.4 Landslide mapping

We identified unstable slopes and mapped scarps, trenches, and fractures on the 2006 orthophoto and the 2015-2016 Lidar DEM. InSAR analysis constrained the

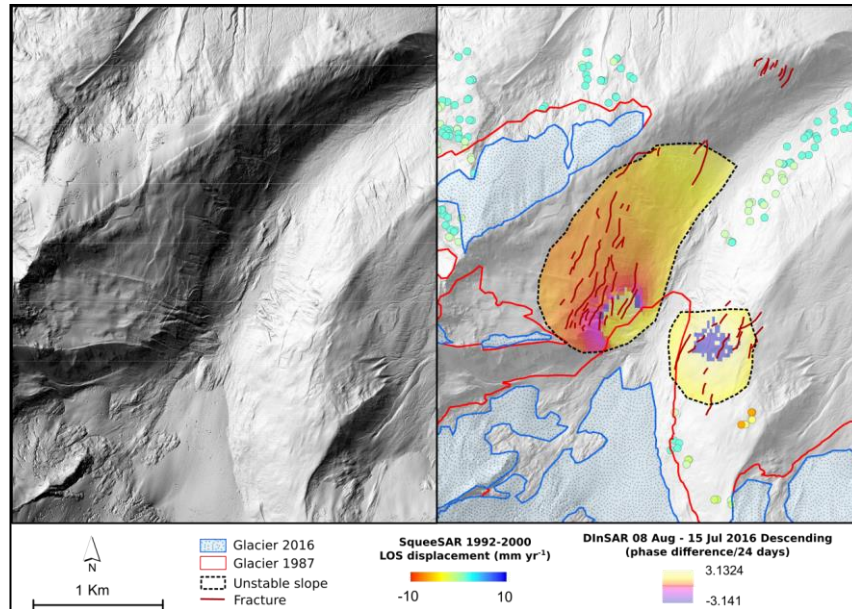


Figure 3. Mosaic Creek valley (Inset B, Figure 1), showing past and present glacier outlines, unstable slopes and fractures. SqueeSAR displacement data, and DInSAR phase difference are also shown. The volume estimate for the unstable west and east flanks is  $10^8$ - $10^9$  m<sup>3</sup> and  $10^6$ - $10^7$  m<sup>3</sup>, respectively. LOS = line of sight

motion on some of the unstable slopes and allowed us to identify other instabilities with less evident geomorphic expression. We have estimated the volumes of these instabilities from their geometry, lithology, and an assumed minimum depth of failure of 100 m (Kilburn and Petley 2003).

### 2.5 Glacier changes 1987-2016

We generated a DEM-of-difference (DoD) by comparing the 1987 Trim and the 2015-2016 LiDAR DEMs. DoD analysis allowed us to detect slope movements and measure glacier extent and mass balance. To assess possible DoD errors we looked at elevation differences in stable areas where the change should be zero. The difference in these areas yielded a  $\sigma_{DoD}$  of 10.7 m. To assess possible errors in volumes we applied the formula  $\sigma_{Vol} = \sigma_{DoD}d^2(n)^{0.5}$  (Lane et al. 2003), where  $d$  is the size of the raster cell and  $n$  the number of cells. The area of ice cover is represented by 331,537 pixels ( $n$ ) of 18.3-m size ( $d$ ). The resulting volumetric uncertainty,  $\sigma_{Vol}$ , is 0.002 km<sup>3</sup>. This would be considered a minimum error because of issues related to digitization and inaccuracy in the TRIM data.

## 3 RESULTS

### 3.1 1987-2016 DEMs comparison

Comparison of the 1987 and 2015-2016 DEM indicated a total ice loss of  $1.3 \pm 0.002$  km<sup>3</sup>. Present ice cover on the massif is about  $28 \times 10^6$  m<sup>2</sup>. Most of the ice loss is in glacier ablation zones and is manifested by significant retreat of glacier termini (Figure 1). Individual glacier

termini have retreated, on average, 15 m yr<sup>-1</sup>; some small glaciers and snowfields disappeared between 1987 and 2016 (Figure 1). Job Glacier downwasted up to 50 m just downflow from an ice fall, near the firn line, where in 2016 fumaroles formed ice caves. Its present area is  $2.7 \times 10^6$  m<sup>2</sup>.

Comparison of the two DEMs revealed a previously unidentified landslide area. The DoD shows loss of mass in the east fork of Devastation Creek valley (7 in Figure 1) and accumulation of material on the valley floor. To better constrain the date of this slope failure, we analyzed available air photos and optical satellite imagery, and found that the landslide occurred between 2006 and 2010. The area of the failure is  $0.2 \times 10^6$  m<sup>2</sup>, and its volume is estimated to be in the range  $10^6$  -  $10^7$  m<sup>3</sup>.

### 3.2 Landslide inventory and InSAR deformation data

Most slopes on the Mt. Meager Volcanic Complex show signs of instability. We identified 27 large ( $>5 \times 10^5$  m<sup>2</sup>) potential landslide sites (Table 1), characterized by cracks, counter scarps, bulging profiles, and small collapses. Cracks generally are parallel to valley axes and exist from the base of the slopes to ridge crests. Of these 27 sites, nine have been deglaciated recently; the toes of the slopes were covered by glacier ice in 1987, but were largely ice-free in 2016. Eight sites are  $>1700$  m a.s.l., where permafrost may be present. Ten sites are at lower elevation in vegetated terrain. We estimate that 12 sites could generate  $10^8$ - $10^9$  m<sup>3</sup> landslides, seven could generate  $10^7$ - $10^8$  m<sup>3</sup> landslides, six  $10^6$ - $10^7$  m<sup>3</sup> landslides, and two  $10^5$ - $10^6$  m<sup>3</sup> landslides (Table 1).

SqueeSAR analysis of the 1992-2000 ERS data, shows motion at four sites (Table 1). The displacement is along the satellite line of sight (LOS) and negative values indicate motion away from the satellite along the 24.9° look angle. LOS displacements of up to  $-17 \text{ mm yr}^{-1}$  were found on the east flank of Job Creek (Inset A in Figure 1, Figure 2). Displacements on the north side of Meager Creek valley are up to  $-12 \text{ mm yr}^{-1}$ , and the southeast side of the valley up to  $-8 \text{ mm yr}^{-1}$ . Displacements on the east side of Mosaic Creek are up to  $-7 \text{ mm yr}^{-1}$  (Inset B in Figure 1, Figure 3).

The Sentinel-1 DInSAR data shows motion at eight sites (Table 1). Displacement occurs for some sites throughout the summer (July-September), while others only move at the beginning of the season (July-August). Specifically, the west and east flanks of Mosaic Creek (Inset B in Figure 1, Figure 3) show movement fringes in the July and August DInSAR results, but not in the August-September period. The east flank of Affliction Creek (Inset C in Figure 1, Figure 4), the east flank of Job Creek (Inset A in Figure 1, Figure 2), and the east flank of Devastation Creek (Inset D in Figure 1, Figure 5), move throughout the summer (July-September). The east flank of Devastation Creek valley is the largest unstable slope we identified ( $3.6 \times 10^6 \text{ m}^2$ ); the second largest unstable slope is the east flank of Job Creek ( $2.7 \times 10^6 \text{ m}^2$ ) (Table 1). We converted the deformation at Job and Devastation creeks from phase information to line-of-sight displacement. Displacements at Job Creek are up to  $-34 \pm 10 \text{ mm}$  and at Devastation are up to  $-36 \pm 10 \text{ mm}$  over a 24-day period in July-August 2016. Collapse of either of these slopes could generate a  $10^8$ - $10^9 \text{ m}^3$  landslide.

Table 1. Inventory of unstable slopes on the Mt. Meager volcano.

Basin	Area ( $\text{m}^2$ )	Volume ( $\text{m}^3$ )	Deglaciaded since 1987?	Motion	
				SSAR	DSAR
Devastation	$3.6 \times 10^6$	$10^8$ - $10^9$	Yes	-	✓
Job	$2.7 \times 10^6$	$10^8$ - $10^9$	Yes	✓	✓
SE Meager	$2.2 \times 10^6$	$10^8$ - $10^9$	No*	✓	-
Meager	$2.1 \times 10^6$	$10^8$ - $10^9$	No	-	-
Meager	$1.6 \times 10^6$	$10^8$ - $10^9$	No	-	-
Devastation	$1.5 \times 10^6$	$10^8$ - $10^9$	No	-	-
Meager	$1.5 \times 10^6$	$10^8$ - $10^9$	No	-	-
Mosaic	$1.4 \times 10^6$	$10^8$ - $10^9$	Yes	-	✓
Affliction	$1.3 \times 10^6$	$10^8$ - $10^9$	Yes	-	-
Manatee	$1.3 \times 10^6$	$10^8$ - $10^9$	No	-	-
Devastation	$1.1 \times 10^6$	$10^8$ - $10^9$	No	-	-
Manatee	$1.0 \times 10^6$	$10^8$ - $10^9$	No	-	-
Devastation	$0.8 \times 10^6$	$10^7$ - $10^8$	Yes	-	✓
N Meager	$0.8 \times 10^6$	$10^7$ - $10^8$	No*	✓	-
Capricorn	$0.7 \times 10^6$	$10^7$ - $10^8$	No	-	-
Meager	$0.6 \times 10^6$	$10^7$ - $10^8$	No	-	-
Job	$0.6 \times 10^6$	$10^7$ - $10^8$	Yes	-	-
Affliction	$0.5 \times 10^6$	$10^7$ - $10^8$	Yes	-	✓
Devastation	$0.5 \times 10^6$	$10^7$ - $10^8$	No*	-	-
Mosaic	$0.4 \times 10^6$	$10^6$ - $10^7$	Yes	✓	✓
Lillooet	$0.4 \times 10^6$	$10^6$ - $10^7$	No*	-	-
Capricorn	$0.3 \times 10^6$	$10^6$ - $10^7$	No	-	-
Devastation	$0.3 \times 10^6$	$10^6$ - $10^7$	Yes	-	✓
Job	$0.3 \times 10^6$	$10^6$ - $10^7$	No*	-	-
Devastation	$0.3 \times 10^6$	$10^6$ - $10^7$	No*	-	✓
Job	$0.1 \times 10^6$	$10^5$ - $10^6$	No*	-	-
Job	$5 \times 10^5$	$10^5$ - $10^6$	No*	-	-

Notes: Volume estimates are based on geometry, lithology, and a minimum depth of failure of 100 m. SSAR = SqueeSAR. DSAR = DInSAR. SE= southeast. N = north. \*Above vegetation limit, possible permafrost.

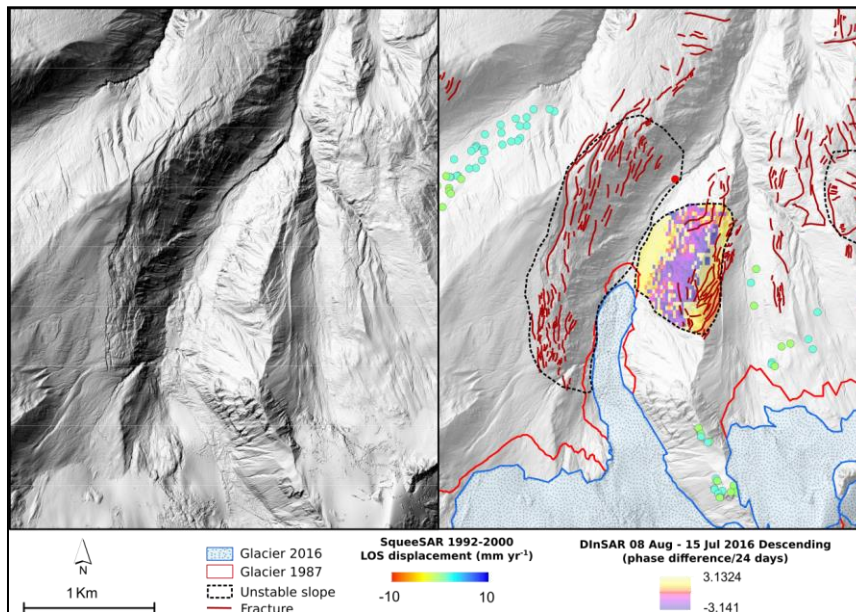


Figure 4. Affliction Creek valley (Inset C, Figure 1), showing past and present glacier outlines, unstable slopes, fractures, SqueeSAR displacement data, and DInSAR phase difference. The volume estimate is of  $10^8$ - $10^9 \text{ m}^3$  and  $10^7$ - $10^8 \text{ m}^3$  for the west and east flanks respectively LOS = line of sight.

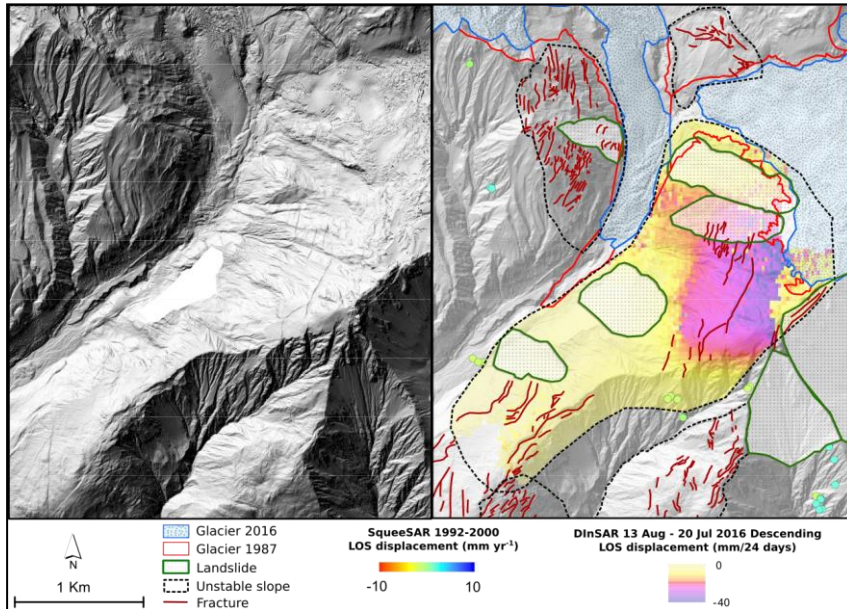


Figure 5. Inset D in Figure 1. The Devastation Creek valley showing past and present glacier outlines, unstable slopes, fractures, SqueeSAR displacement data, and DInSAR deformation map. The volume estimate is of  $10^8$ - $10^9$  m<sup>3</sup>. LOS = line of sight

## 4 DISCUSSION

### 4.1 Glacial retreat at Mt Meager volcano

The Mt. Meager volcano has lost 1.3 km<sup>3</sup> of ice since 1987. The scale of deglaciation is comparable to that elsewhere in the Coast Mountains and in other high mountains around the world. If climate continues to warm, as is likely, most glaciers at Mt. Meager will have disappeared by the end of this century (Bolch et al. 2010, Clarke et al. 2015).

### 4.2 Volcano-ice interaction hazards

In 2016 fumaroles were observed emitting gases from Job Glacier. The fumaroles have probably been active beneath the glacier for a long time, but only recently has the ice thinned enough that the hot gases could reach the surface of the glacier. The hazard posed directly by the gases is localized to the ice caves and immediate surroundings. The possibility of an eruption from the volcano is unknown, but ice melt can cause landslides and de-compression from both ice loss and landslides might destabilize hydrothermal and magmatic systems and trigger an eruption (cf Waythomas 2012). Even a small eruption would rapidly melt a large amount of Job Glacier ice, generating a long run-out debris flow. A tragic example of such an event is the 1985 eruption of Nevado del Ruiz in Colombia. A small eruption beneath the summit ice-cap caused a debris flow that killed more than 22,000 people over 60 km from the volcano (Herd et al. 1986). At present no volcanic or volcano-ice interaction hazard assessments have been made for Mt. Meager.

### 4.3 Landslide hazards

Of the 27 slopes with signs of instability that we identified, nine slopes have been recently deglaciated and eight are at elevations where permafrost degradation is likely to be happening. Glacier retreat and permafrost thaw could destabilize these slopes. Meltwater from snow and ice can infiltrate slopes and increase porewater pressures, conditioning them for catastrophic collapse, as happened at Mt. Meager in 2010. Hetherington (2014) conducted edifice-scale slope stability analysis using numerical modeling and showed that that even small changes in water supply could trigger deep-seated failure. The calculated factor of safety (FOS) showed that many sites are at incipient failure.

Collapses of these slopes can generate highly mobile, far-reaching debris flows. Five of the unstable slopes we identified could generate a  $10^8$ - $10^9$  m<sup>3</sup> debris flow that might reach populated areas in the Lillooet River valley (four past documented events: 2600, 4400, 6250, 7900 BP) Another five slopes could generate landslides with volumes of  $10^7$ - $10^8$  m<sup>3</sup> that might extend some distance down Lillooet valley (three past documented events: 2170 BP, 1975, 2010). Five more could generate a  $10^6$ - $10^7$  m<sup>3</sup> flow that could reach downstream of the Meager-Lillooet confluence (1860, 870, 370 BP; 1931, 1998), and two sites have volumes of  $10^5$ - $10^7$  m<sup>3</sup> and would likely be confined in the proximal valleys of Meager Creek and upper Lillooet River. See Simpson et al. 2006 for the inundation zones extents and Friele et al. 2008 for a compilation of past events. Ten slopes are forested and have not been directly affected by recent deglaciation; we consider these slopes less likely to generate catastrophic collapses. Seven of them have volumes in the  $10^8$ - $10^9$  m<sup>3</sup>

range, two in the  $10^7$ - $10^8$  m<sup>3</sup> range, and one in the  $10^6$ - $10^7$  m<sup>3</sup> range. Three of the vegetated slopes (southeast Meager and east Manatee valley sides) are not underlain by volcanic rocks.

#### 4.4 InSAR deformation data

ERS SqueeSAR data provided valuable historic information spanning an 8-year period while the Sentinel-1 DinSAR data provided short-term data during the summers of 2015 and 2016. The ERS analysis showed motion on four slopes, with rates up to  $-17$  mm yr<sup>-1</sup> at Job Creek. Analysis of Sentinel-1 data showed motion on eight slopes, including deformation of about 35 mm over a 24-day period on the east flanks of Job and Devastation creeks (Figure 2 and 5). The Job and Devastation Creek slopes are of particular concern as they have been recently deglaciated and have large open fractures indicative of precursory collapse. Our catalogue of deforming slopes is likely incomplete; more slopes might be deforming and be in critical condition but are not visible due to adverse satellite look angles, the presence of vegetation or snow cover.

#### 4.5 Risk from landslides and volcanic activity at Mt. Meager

Friele et al. (2008) deemed the risk of loss of life from a large landslide from Mt. Meager to be unacceptable. This conclusion was based on an analysis of the frequency and size of past landslides and their runout and combined with a consideration of acceptable risk criteria for landslides in other jurisdictions. In view of the history of landslides on the massif, including the 2010 landslide, future collapses are certain. This inevitability must be considered in view of the recent increase in infrastructure near Mt. Meager and the increase in population and related infrastructure in the Pemberton area. Today, two hydropower plants, a new access road, and mining operations are in the range of  $10^6$ - $10^7$  m<sup>3</sup> debris flows. Homes, roads, and bridges are in the range of  $10^9$  m<sup>3</sup> debris flows. The only active risk mitigation strategy is restriction of public and industrial users from upper Lillooet River valley during high and extreme weather conditions (Cordilleran Geoscience 2012). There is a water-level gauge on the Lillooet River 35 km downstream from the volcano, which might alert residents to sudden changes in the discharge of the river, such as a drop in flow caused by formation of a landslide dam. However, this gauge is remote from the proximal zone of a potential catastrophic slope failure, resulting in a warning delay of several hours. Furthermore, different mechanisms that might cause a rapid increase in river level (e.g. normal flood or a surge) cannot be easily resolved. Therefore, there is no early warning system or defensive structures that might reduce the risk to the population downstream of Mt. Meager.

#### 4.6 Slope monitoring and early warning system

Although non-eruptive volcanic landslides are difficult to predict, Roberti et al (2017c) showed that the 2010 Mt.

Meager landslide should not have been unexpected. Signs of deformation were evident on the pre-failure slope, and slope monitoring might have allowed the landslide to have been forecast (Intrieri et al. 2017). In this study, we have identified additional unstable slopes and have measured displacement rates with InSAR techniques. To reduce the risk of injury and loss of life from landslides at Mt. Meager, we recommend the establishment of slope deformation monitoring and an early warning system. Both can be achieved using satellite InSAR. InSAR allows precise displacement monitoring over large areas in near-real time, making the technique suitable for an early warning system (Ferretti et al. 2015; Intrieri et al. 2017). The availability of free Sentinel imagery with near worldwide coverage has the potential to significantly boost this type of application. The main limitations in the use of InSAR are slope geometry and the loss of coherence in areas covered by snow and forest. Most of the slopes of concern at Mt. Meager, such as the east flank of Job Creek valley and the east flank of Devastation Creek valley, have favourable orientations for displacement detection (E-W). Despite the area being covered by snow for most of the year, deformation can be detected during the summer season, when movements are expected to be greatest and when the human presence near Mt. Meager is more common. Other remote and ground-based methods can be integrated into an InSAR monitoring system. Optical satellite imagery and aerial Lidar data can provide information on deformation rates in areas of unsuitable InSAR geometry. Photogrammetry, Lidar, and ground-based GPS can be employed to monitor slopes considered to be most hazardous. Automated photogrammetric stations are inexpensive and can be integrated with periodical (weekly/monthly) terrestrial Lidar surveys. Direct GPS slope instrumentation is an established technique, but in this case involves a high risk of instrument loss. Sensors could also be installed in the major valleys (Devastation, Job, Capricorn, Mosaic, and Affliction) and in Lillooet River valley to provide warnings of collapses. Numerical modelling can be applied to better constrain the possible runouts and to develop hazard maps.

## 5 CONCLUSIONS

DEMs, Lidar, SfM, InSAR analysis, and field work allowed us to document glacier retreat and slope instability on the Mt. Meager volcanic complex. We draw the following conclusions:

- 1) Mt. Meager volcano has lost  $\sim 1.3$  km<sup>3</sup> since 1987. Present-day glacier cover is  $28 \times 10^6$  m<sup>2</sup>
- 2) In 2016 fumaroles were observed in Job Glacier. Although the hazard from volcanic gases is localized, an eruption under the glacier would melt a large volume of ice and generate far-reaching debris flows. Further studies are needed to better constrain the possibility of a volcanic eruption at Mt. Meager.
- 3) We have documented 27 large ( $> 5 \times 10^5$  m<sup>2</sup>), potentially unstable sites, 17 of which have become ice-free recently. Fifteen of the slopes have volumes  $> 10^6$  m<sup>3</sup>; if they were to fail catastrophically,

infrastructure near the volcano might be affected. Ten have volumes  $>10^7$  m<sup>3</sup>; their failure might impact populated areas downstream.

- 4) InSAR is an invaluable resource to study slope instabilities. The 1992-2000 ERS SqueeSAR analysis identified ground motion at four sites. The east flank of the valley of Job Creek moved at  $-17$  mm yr<sup>-1</sup> over the 8-year period. 2015 and 2016 Sentinel-1 DInSAR data highlighted motion at eight sites. Among these, the east slopes of Job Creek and Devastation Creek valleys moved up to  $-34\pm 10$  mm  $-36\pm 10$  mm, respectively, over a 24-day period during the summer of 2016. We consider these slopes to be in a critical condition for failure.
- 5) The risk of loss of life was deemed unacceptable in 2008. Today, in a first-order estimate, the risk has increased.
- 6) An InSAR-based slope monitoring and early warning system should be implemented at Mt. Meager volcano to mitigate the high level of risk.

## 6 ACKNOWLEDGMENTS

Financial support for the 2015 LiDAR data acquisition was provided by NSERC through Discovery Grants to Clague and Menounos and the Canada Foundation for Innovation (Menounos). Natural Resources Canada (NRCan), through Melanie Kelman, provided funds for the 2016 Lidar data set. Fieldwork was supported by Chairs grants to Ward. The InSAR analyses were provided by TRE-Altamira.

## 7 REFERENCES

- Bakker, M. and Stuart, N.L. 2016. Archival Photogrammetric analysis of river-floodplain systems using Structure from Motion (SfM) methods, *Earth Surface Processes and Landforms*, 42: 1274–1286, doi:10.1002/esp.4085.
- Bolch, T. Menounos, B. and Wheate, R. 2010. remote Sensing of Environment Landsat-Based Inventory of Glaciers in Western Canada, 1985 – 2005. *Remote Sensing of Environment* 114 (1), 127–37. doi:10.1016/j.rse.2009.08.015.
- Carrivick, J.L. Smith, M.W. and Quincey, D.J. 2016. *Structure from Motion in Geosciences*, John Wiley & Sons, Pondicherry, India.
- Clague, J.J. Evans, S.G. Rampton, V.N. and Woodsworth, G.J. 1995. Improved age estimates for the White River and Bridge River tephra, western Canada, *Canadian Journal of Earth Sciences*, 32: 1172–1179, doi:10.1139/e95-096.
- Clague, J.J. and Ward, B. 2011. Pleistocene glaciation of British Columbia. In Ehlers, L. Gibbard, P.L. and Hughes, P.D. (eds.), *Quaternary glaciations—extent and chronology: a closer look. Developments in Quaternary Science* 15, Elsevier, Amsterdam, Netherlands, p. 563– 573. <https://doi.org/10.1016/B978-0-444-53447-7.00044-1>
- Clarke, G. K.C Jarosch, A. H. Anslow, F. S. Radich, V. and Menounos, B. 2015. Projected deglaciation of western Canada in the in the 21st century. *Nature Geoscience* 8:372–377. <https://doi.org/10.1038/NGEO2407>
- Cordilleran Geoscience 2012. *Volcanic Landslide Risk Management, Lillooet River Valley, BC: Start of North and South FSRs to Meager Confluence, Meager Creek and Upper Lillooet River*. Report to Squamish District, Ministry of Forests, Lands and Natural Resource Operations,
- Ferretti, A. Fumagalli, A. Novali, F. Prati, C. Rocca, F. and Rucci, A. 2011. A new algorithm for processing interferometric data- stacks: SqueeSAR, *IEEE Transactions on Geosciences and Remote Sensing* 49: 3460–3470.
- Ferretti, A. Davide, C. Fumagalli, A. Novali, F. and Rucci, A. 2015. InSAR data for monitoring land subsidence: Time to think big, *Proceedings of the International Association of Hydrological Sciences*, 92(1): 1–4, doi:10.5194/piahs-372-331-2015.
- Fonstad, M.A. Dietrich, J.T. Courville, B.C. Jensen, J.L. and Carbonneau, P.E. 2013. Topographic structure from motion: A new development in photogrammetric measurement, *Earth Surface Processes and Landforms*, 38; 421–430, doi:10.1002/esp.3366,
- Friele, P.A. and Clague, J.J. 2004. Large Holocene landslides from Pylon Peak, southwestern British Columbia, *Canadian Journal of Earth Sciences*, 41; 165–182
- Friele, P.A. Clague, J.J. Simpson, K. and Stasiuk, M. 2005. Impact of a Quaternary volcano on Holocene sedimentation in Lillooet River valley, British Columbia, *Sedimentary Geology*, 176: 305–322
- Friele, P. Jakob, M. and Clague, J.J. 2008. Hazard and risk from large landslides from Mount Meager volcano, British Columbia, Canada. *Georisk: Assessment and management of Risk for Engineered Systems and geohazards* 2: 48–64, <https://doi.org/10.1080/17499510801958711>
- Gomez, C. Hayakawa, Y and Obanawa, H. 2015. A study of Japanese landscapes using Structure from Motion derived DSMs and DEMs based on historical aerial photographs: New opportunities for vegetation monitoring and diachronic geomorphology, *Geomorphology*, 242: 11–20, doi:10.1016/j.geomorph.2015.02.021.
- Herd, D.G. and the Comité de Estudios Vulcanológicos. 1986. The 1985 Ruiz volcano disaster. *EOS, Transactions of the American Geophysical Union*, 67: 457–460

- Hetherington, R. M. 2014. *Slope stability analysis of Mount Meager, south-western British Columbia, Canada*. M.Sc. thesis, Michigan Technological University, Houghton, Michigan, 68 p.
- Hickson, C.J. Russell, J.K. and Stasiuk, M.V. 1999. Volcanology of the 2350 B.P. Eruption of Mount Meager Volcanic Complex, British Columbia, Canada: Implications for hazards from eruptions in topographically complex terrain, *Bulletin of Volcanology*, 60:489–507.
- Holm, K. Bovis, M. and Jakob, M. 2004. The landslide response of alpine basins to post-Little Ice Age glacial thinning and retreat in southwestern British Columbia *Geomorphology*, 57: 201–216.
- Intrieri, E. Raspini, F. Fumagalli, A. Lu, P. Del Conte, S. Farina, P. Allievi, J. Ferretti, A. and Casagli, N. 2017. The Maoxian landslide as seen from space: Detecting precursors of failure with Sentinel-1 data, *Landslides*: 15:123–133, doi:10.1007/s10346-017-0915-7.
- James, M.R. and Robson, S. 2012. Straightforward reconstruction of 3D surfaces and topography with a camera: Accuracy and geoscience application: *Journal of Geophysical Research*, 117, F03017, doi:10.1029/2011JF002289 .
- Jakob, M. 1996. *Morphometric and Geotechnical Controls on Debris Flow Frequency and Magnitude, Southern Coast Mountains, British Columbia*. Ph.D. thesis, University of British Columbia, Vancouver, BC, 242 p.
- Jakob, M. 2005. A size classification for debris flows. *Engineering Geology*, 79; 151–161.
- Jordan, P. 1994. *Debris Flows in the Southern Coast Mountains, British Columbia: Dynamic Behaviour and Physical Properties*. Ph.D. thesis, University of British Columbia, Vancouver, BC, 260 p.
- Kilburn, C.R.J. and Petley, D.N. 2003. Forecasting giant, catastrophic slope collapse: lessons from Vajont, Northern Italy. *Geomorphology* 54:21–32. [https://doi.org/10.1016/S0169-555X\(03\)00052-7](https://doi.org/10.1016/S0169-555X(03)00052-7)
- Koch, J. Menounos, B. and Clague, J.J. 2009. Glacier change in Garibaldi Provincial Park, southern Coast Mountains, British Columbia, since the Little Ice Age. *Global and Planetary Change*, 66: 161–178, <https://doi.org/10.1016/j.gloplacha.2008.11.006>.
- Lane, S. N. Westaway, R. M. and Hicks, M. D. 2003. Estimation of Erosion and Deposition Volumes in a Large, Gravel-Bed, Braided River Using Synoptic Remote Sensing. *Earth Surface Processes and Landforms*, 28 (3): 249–71. doi:10.1002/esp.483.
- Leroi, E. Bonnard, Ch. Fell, R. and McInnes, R. 2005. Risk assessment and management. Proceedings of the International Conference on Landslide Risk Management, Vancouver, BC, 159–198
- Read, P. B. 1978. Geology of Meager Creek Geothermal Area, British Columbia. *Geological Survey of Canada Open File 603*, map, 1 sheet, scale 1:20000
- Roberti, G. Friele, P. van Wyk De Vries B., Ward, B. Clague J.J., Perotti, L. and Giardino, M. 2017a. Rheological evolution of the Mount Meager 2010 debris avalanche, southwestern British Columbia. *Geosphere*, 13: 1–22, doi:10.1130/GES01389.1.
- Roberti, G. Ward, B. Van Wyk De Vries, B. and Perotti, L. 2017b. Structure from Motion and landslides: The 2010 Mt Meager collapse from slope deformation to debris avalanche deposit mapping. *Geotechnical News*, 35: 20–24.
- Roberti, G. Ward, B. Van Wyk De Vries, B. Friele, P.A. Perotti, L. Clague, J.J. and Giardino, M. 2017c. Precursory slope distress prior to the 2010 Mount Meager landslide, British Columbia. *Landslides*. 1-11, doi:10.1007/s10346-017-0901-0.
- Simpson, K.A. Stasiuk, M. Shimamura, K. Clague, J.J. and Friele, P. 2006. Evidence for catastrophic volcanic debris flows in Pemberton Valley, British Columbia. *Canadian Journal of Earth Sciences*, 43: 679–689, doi:10.1139/E06-026.
- Statistics Canada. 2017. *Pemberton [Population Centre], British Columbia and British Columbia [Province] (table)*. *Census Profile. 2016 Census. Statistics Canada Catalogue no. 98-316-X2016001*. Ottawa, ON. Released November 29, 2017.
- Venugopal, S. Moune, S. William-Jones, G. Wilson, A. and Russel, K. 2017. Gas emissions and magma source of the Mount Meager Volcanic Complex, Garibaldi Volcanic Belt, BC., *IAVCEI Scientific Assembly Abstracts, August 14-18, 2017, Submission 244*, Portland, OR.
- Waythomas, C. 2012. Landslides at stratovolcanoes initiated by volcanic unrest. In Clague, J.J. and Stead, D. (eds.), *Landslides: Types, Mechanisms and Modeling* (pp. 37-49). Cambridge: Cambridge University Press, doi:10.1017/CBO9780511740367.005.
- Westoby, M.J. Brasington, J. Glasser, N.F. Hambrey, M.J. and Reynolds, J.M. 2012. 'Structure-from-Motion' photogrammetry: A low-cost, effective tool for geoscience applications, *Geomorphology*, 179: 300–314, doi:10.1016/j.geomorph.2012.08.021.